

Calibration of Tests for Time Dilation in GRB Pulse Structures

J.P. Norris,¹ R.J. Nemiroff,² J.T. Bonnell,³ and J.D. Scargle⁴

¹NASA/Goddard Space Flight Center, Greenbelt, MD 20771

²George Mason University, Fairfax, VA 22030

³Universities Space Research Association

⁴NASA/Ames Research Center, Moffett Field, CA 94035

Two tests for cosmological time dilation in γ -ray bursts – the peak alignment and auto-correlation statistics – involve averaging information near the times of peak intensity. Both tests require width corrections, assuming cosmological origin for bursts, since narrower temporal structure from higher energy would be redshifted into the band of observation, and since intervals between pulse structures are included in the averaging procedures. We analyze long (> 2 s) BATSE bursts and estimate total width corrections for trial time-dilation factors ($TDF = [1+z_{\text{dim}}]/[1+z_{\text{brt}}]$) by time-dilating and redshifting bright bursts. Both tests reveal significant trends of increasing TDF with decreasing peak flux, but neither provides sufficient discriminatory power to distinguish between actual TDFs in the range 2–3.

TWO WIDTH CORRECTIONS TO OBSERVED TIME DILATION

If γ -ray bursts (GRB) are at cosmological distances, then the temporal structure associated with each energy range at the source is shifted to lower energies in the observer's frame of reference. Since GRB pulse structures are narrower at higher energy, this redshift-dependent *narrowing* would compete with cosmological time dilation. Note that both redshift-dependent narrowing and time dilation have mathematical analogues in special relativistic (SR) beaming models – blue-shifting of the radiation, and time contraction of the temporal structure. So far, there is no observational data which affords a way to distinguish between SR and cosmology in GRBs. We discuss the problem in terms of the cosmological hypothesis, keeping in mind that both cases have the same temporal mensuration problems.

Each measure of time dilation in GRBs requires a different width correction for narrowing of temporal structure, but all such corrections operate in the same sense: The *actual* time-dilation factor (TDF) is decreased by the redshift effect, so that the *observed* TDF, between bright and dim groups of bursts, is smaller, and a function of temporal structure in both groups,

$$TDF_{\text{obs}} = F[TDF_{\text{act}}, \Lambda(TDF_{\text{act}} \times E_c), \Lambda(E_c)] \quad (1)$$

where E_c is the energy band of observation, and $TDF_{\text{act}} \times E_c$ is the band, relative to z_{brt} of bright bursts, from whence the temporal structure was redshifted (1–3). Of course, $TDF_{\text{act}} = [1+z_{\text{dim}}]/[1+z_{\text{brt}}]$ is what we are after. The insidious part is the dependence of Λ , a generic width statistic, on TDF_{act} . Thus the energy-dependent width correction for redshift is like a ratio of widths of temporal structure, but it is not a simple ratio for all time dilation measures, for the following reason: For measures which utilize information from a portion of the time profile that contains any intervals or valleys between pulse structures, time dilation of these regions interjacent to peaks “subtracts” from time dilation of regions of emission, since interval regions and emission regions are not segregated. Thus when these portions of time profiles are averaged – as in Peak Aligned profile (PA) and Auto-Correlation Function (ACF) measures – regions of emission and intervals between pulses are thrown together in the averaging process. The resulting situation is illustrated in Figure 4 of ref (4), in these proceedings.

For the PA and ACF statistics we have calibrated the resulting diminution of time dilation that would arise for the combined effects of redshift of temporal structure and averaging of regions that contain intervals. Note that correction for the latter effect, previously not addressed (1,3), is not required for time-dilation measures which rely upon distributions of a measured parameter, such as distributions of pulse widths, intervals between pulses, or burst durations. Instead, these measures have simple width-correction ratios, that can be obtained from the distributions in two relevant energy bands.

CALIBRATION OF WIDTH CORRECTIONS

The PA and ACF tests for time dilation have been described before (1,3,5). The basic procedures are: divide bursts into groups based on some measure of brightness; and within a brightness group, average the profiles with their highest intensity peaks in registration, or average the profiles’ ACFs. The “common-sense” appeals of the PA test are that it operates entirely in the time domain, and makes use of the most intense part of a burst. The efficacy of the ACF test is that it probes short timescales, to the limit of temporal resolution, without the need to worry about finding the exact location of peak intensity in dim bursts. Also, the ACF has a well-defined correction for co-added noise at zero lag. For both tests the main problem is that the width corrections are appreciable, resulting in less than satisfactory discriminatory power in the TDF_{act} range ~ 2 –3, given the present sample variance.

Data preparation. We use BATSE DISCSC data summed over channels 1 and 2 (~ 27 –115 keV) to construct average peak-aligned profiles and ACFs for bursts longer than ~ 2 s and with peak intensities higher than 1400 counts s^{-1} .

The bursts are divided into six brightness groups, ~ 85 bursts per group, according to their BATSE 3B peak fluxes determined at 256 ms. This timescale compromises between 64 ms, where noisier estimates are obtained for dim bursts, and 1024 ms, which integrates over pulse widths (pulses in long bursts having FWHM ~ 100 –500 ms, dependent on energy band (6)). Quadratic (infrequently, higher order) backgrounds are fitted and subtracted. For the PA test the time profiles are rendered to 512-ms resolution; the original 64-ms resolution is preserved for the ACF test. To approximately nullify brightness bias, the comparison of average profiles or ACFs between different brightness groups (described below) is performed with the signal-to-noise (s/n) levels of the individual time profiles of the bright group equalized to the s/n levels of the profiles of the other groups. For each of the five brightness groups below the brightest, ten such noisy realizations per bright burst are computed, with the new peak intensity chosen randomly from among the peak intensities of the bursts of each respective group. Thus, about $850 \times 5 = 4250$ noisy realizations of bright bursts are created.

Estimating observed time dilation. For -8 to +16 (512-ms) bins of the peak of the average PA profiles of the bright bursts, the intensity levels and corresponding profile widths for a dimmer group are found, and width ratios computed for the 24 bins (N_{PA}). A similar procedure is followed for the ACFs, for ± 60 64-ms lag bins (N_{ACF}). However, since pulse widths (FWHM) in individual bursts are ~ 500 ms, only $N_{\text{indep}} \approx 12$ and 4 independent ratio estimates result for PA and ACF procedures, respectively. We estimate means, standard and sample errors by a bootstrap procedure (7). The ~ 85 burst profiles (or ACFs) in each brightness group (850 noisy realizations for the brightest group) are considered the “parent population” from which 85 profiles are drawn randomly with replacement. For each brightness group the random selection is repeated 500 times. For each run the average profile is computed, and the width ratios computed as described above. The $500 \times N_{\text{PA}}$ (or N_{ACF}) width ratios are rank ordered. The resulting 50th, 15nd, and 84th percentile levels are taken as the median width ratio – box symbols in Figures 1 and 2 – negative and positive $1\text{-}\sigma$ standard errors, respectively. The sample errors plotted are these $1\text{-}\sigma$ errors reduced by the factor $\sqrt{N_{\text{indep}}}$.

For the PA and ACF measures, the *observed* TDFs range up to ~ 1.75 and ~ 1.45 , respectively, for the dimmest group relative to the brightest. But the *actual* TDFs would be larger in both the cosmological and SR beaming hypotheses, by width-correction factors we estimate as follows.

Estimating width corrections, interval dilation+redshift effects. The expected time-dilation “signal”, *sans* redshift effect, is easily simulated by merely stretching the profiles (using the original 64-ms data) of the bright group by factors of 2.0 and 3.0, and comparing with the unstretched profiles, but now using 16-channel MER data. For *actual* TDFs of 2.0 and 3.0, the *recovered* TDFs for the PA measure are ~ 1.7 (85%) and ~ 2.55 (85%), respectively (circle symbols, Figure 1). Similarly for the ACF measure, the recovered TDFs are ~ 1.6 (80%) and ~ 2.0 (66%), respectively (circle symbols, Figure 2).

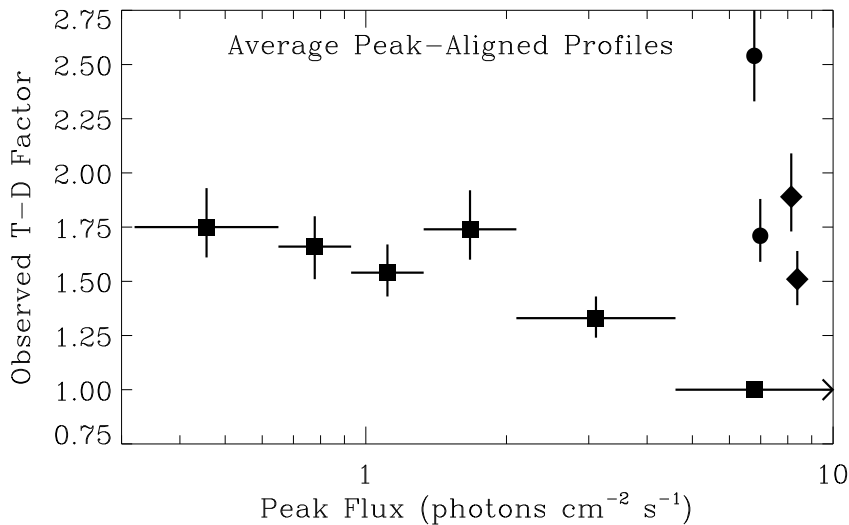


FIG. 1. Box symbols indicate observed time-dilation factor vs. BATSE 3B peak flux (256 ms), determined from average peak-aligned profiles. Errors estimated by bootstrap method. On right side, upper four points (without horizontal bars) are the bright burst sample time-dilated (circle symbols) and then redshifted as well (diamond symbols), by factors of 2 and 3 (lower and upper symbols, respectively). Approximately 85 bursts per group.

Incomplete recovery of the input TDF is attributable to inclusion of regions which contain stretched intervals as well as stretched pulse structures.

Recall that we analyzed the six brightness groups in the 25–115 keV band (box symbols, Figures 1 and 2). The additional effect of redshift of temporal structure is simulated by using the 16-channel data for bright bursts: corresponding approximately to TDF=1, Σ chans: 2–6, \sim 22–100 keV; TDF=2, Σ chans: 4–8 + half of 9, \sim 41–200 keV; and TDF=3, Σ chans: half of 5 + 6–10, \sim 65–315 keV. The combined effect of stretching and redshifting profiles of bright bursts is indicated by diamond symbols in Figures 1 and 2. Narrower structure redshifted into the band of observation further reduces the observed TDF. For actual TDFs and redshifts of 2.0 and 3.0, the recovered TDFs are now \sim 1.5 (75%) and \sim 1.9 (63%), respectively, for the PA measure; the corresponding values for the ACF measure are \sim 1.4 (70%) and \sim 1.6 (54%), respectively. As can be seen by comparing the pairs of diamond symbols (Figures 1 and 2) with the observed TDF determinations for the six brightness groups, the uncertainties are such that TDF_{act} is only constrained to the range \sim 2–3 for the dimmer groups via both the PA and ACF measures.

In conclusion, on the short (64 ms – few s) and intermediate (1–20 s) timescales probed by the PA and ACF tests, observed TDFs, relative to bright bursts, range up to \sim 1.45 (ACF) and \sim 1.75 (PA). From calibrations using the

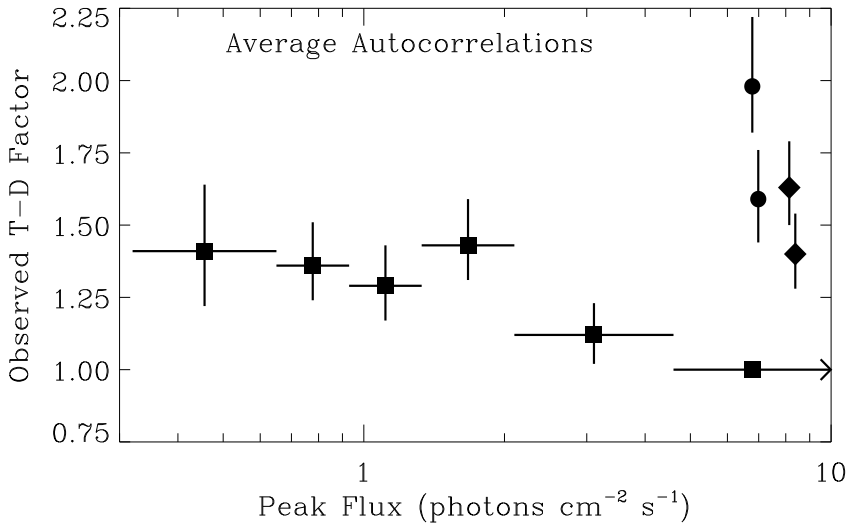


FIG. 2. Similar to Figure 1, except determined from the ACFs of bursts in six brightness groups. Observed TDFs (boxes) are lower than for peak-aligned profiles, but calibrations obtained by time-dilating (circles) and then redshifting (diamonds) bright bursts by factors of 2 and 3 are lower as well. Relatively larger error bars result than for PA measure since fewer independent time bins were used.

bright sample we conclude that, for the same input time-dilation and redshift factor, the ACF *is expected* to yield smaller TDF_{obs} . In fact, actual cosmological TDFs would be somewhat larger than TDF_{obs} : Two effects, redshift of narrower structure into the band of observation, and inclusion of stretched intervals, result in smaller observed time-dilation factors. The second effect was not appropriately simulated in previous estimates which used ratios of average pulses (1) or ratios of average ACFs (3) in different energy bands of bright bursts. The width corrections are more pronounced at higher TDFs, such that with present uncertainties, both the PA and ACF measures only constrain $TDF_{\text{act}} = [1+z_{\text{dim}}]/[1+z_{\text{brt}}]$ to lie in the range 2–3.

REFERENCES

1. J.P. Norris, *et al.*, ApJ **424**, 540 (1994).
2. J.P. Norris, Ap Space Sci **231**, 95 (1995).
3. E.E. Fenimore and J.S. Bloom, ApJ **453**, 25 (1995).
4. J.P. Norris, these proceedings.
5. I.G. Mitrofanov, Ap Space Sci **231**, 103 (1995).
6. J.P. Norris, *et al.*, ApJ **459**, in press (1996).
7. B. Efron and R.J. Tibshirani, *An Introduction to the Bootstrap*, (New York: Chapman and Hall) (1993).